

Synthesis, Structures, and Properties of Two New Two-Photon Photopolymerization Initiators

Yun-Xing Yan,* Xu-Tang Tao, Yuan-Hong Sun,[1] Wen-Tao Yu, Gui-Bao Xu, Chuan-Kui Wang,[1] Hua-Ping Zhao, Jia-Xiang Yang, Xiao-Qiang Yu, Xian Zhao, and Min-Hua Jiang

State Key Laboratory of Crystal Materials, Shandong University, Jinan 250100, P. R. China

[1]Department of Physics, Shandong Normal University, Jinan 250014, P. R. China

Received June 29, 2004; E-mail: yxyan@icm.sdu.edu.cn

Two new two-photon photopolymerization initiators, diphenyl-(4-{2-[4-(2-pyridin-4-ylvinyl)phenyl]vinyl}phenyl)amine **3** and 9-(4-{2-[4-(2-pyridin-4-ylvinyl)phenyl]vinyl}phenyl)-9*H*-carbazole **4**, have been synthesized and their crystal structures have been determined. One-photon fluorescence, one-photon fluorescence quantum yields, one-photon fluorescence lifetimes, and two-photon fluorescence have been investigated. The results show that they are good two-photon absorbing chromophores and effective two-photon photopolymerization initiators. The calculated two-photon absorption cross sections of molecules **3** and **4** for the lowest excited state are 59.3×10^{-50} and 43.0×10^{-50} $cm^4\,s\,photon^{-1}$, respectively. Two-photon initiating polymerization microfabrication experiments have been studied and the possible photopolymerization mechanisms have been discussed.

Molecular excitation via the simultaneous absorption of two photons can lead to improved three-dimensional (3D) control of photochemical or photophysical processes due to the quadratic dependence of the absorption probability on the incident radiation intensity, thus furnishing development of improved 3D microfabrication,[1–6] ultra-high-density optical data storage,[7] biological imaging,[8] and the controlled release of biologically relevant species.[9] Although 3D microfabrication has been illustrated using the two-photon-initiated polymerization of resins incorporating conventional ultraviolet-absorbing initiators, the two-photon absorption (TPA) cross sections (δ) of these initiators are typically very small ($\delta \leq 10 \times 10^{-50}$ cm^4 s per photon), and as a result they exhibit low two-photon sensitivity. Resins containing these initiators can be patterned only by means of long exposure time and high excitation intensities that frequently result in damage to the structure. Although some approaches to improve the photosensitivity of photointiator molecules have been reported, such as improving the two-photon cross section (δ) and the photochemical quantum yield (Φ) of the molecule,[10–13] effective two-photon photopolymerization initiators are still rare because the photopolymerization mechanism and the relationship of the structure/property for the initiator, which is important for searching for effective and high photosensitive two-photon photopolymerization initiators, remains unclear so far.

In our previous work, we had reported an acceptor–π-donor (D–π-A) type of molecule DBASVP that was found to have a large TPA cross section, and to effectively initiate polymerization through two-photon absorption.[14] In the present work, we describe the design and synthesis of two new two-photopolymerization initiators, **3** and **4**, in which the *N*,*N*-dibutylamino group in DABSVP was replaced by *N*,*N*-diphenylamino and *N*-carbazoyl groups, respectively. Our results demonstrate that they were good two-photon absorbing chromophores and effective two-photon photopolymerization initiators. Their cross sections were calculated to be as high as the so-called AF-50.[15] The crystal structures of **3** and **4** were determined to be in the $P2_1$ and $P\bar{1}$ space groups, respectively.

Experimental

Instruments. The 600 MHz ^{1}H NMR spectra and ^{13}C NMR were obtained on a Bruker av600 spectrometer. Elemental analyses were performed using a PE 2400 elemental analyzer. UV–vis–near-IR spectra were measured on a Hitachi U-3500 recording spectrophotometer. Melting points were measured on DSC822^e Mettler-Toledo instruments. The steady-state fluorescence spectra measurements were performed using an Edinburgh FLS 920 spectrofluorimeter. A 450 W Xe arc lamp provided a ~400 nm excitation source. Spectra were record between 420 and 700 nm using a photomultiplier tube as a detector, which was operated in the single-photon counting mode. The spectral resolution was 0.1 nm. The quartz cuvettes used were of 1 cm path length.

Synthesis. The synthetic approaches of **3** and **4** are shown in Scheme 1. 4-bromobenzyl(triphenyl)phosphonium bromide and 4-carbazol-9-ylbenzaldehyde were synthesized according to reported methods.[14,16]

{4-[2-(4-Bromophenyl)vinyl]phenyl}diphenylamine 1: At room temperature, 4-(*N*,*N*-diphenylamino)benzaldehyde (2.73 g, 0.01 mol), 4-bromobenzyl(triphenyl)phosphonium bromide (7.68 g, 0.015 mol), NaOH (8.00 g, 0.2 mol) and THF (2 mL) were added into a mortar. The mixture was then ground, and became orange after five minutes. The mixture was poured into 200 mL of distilled water, neutralized with dilute hydrochloric acid, and extracted with dichloromethane. The obtained organic layer was dried over anhydrous magnesium sulfate. The solvent was removed under reduced pressure and the crude product was purified by column chromatography on silica gel using petroleum ether as the eluent. After removal of the solvent, a pure green product was obtained in 75% yield after recrystallization from ethyl acetate.

Published on the web February 11, 2005; DOI 10.1246/bcsj.78.300

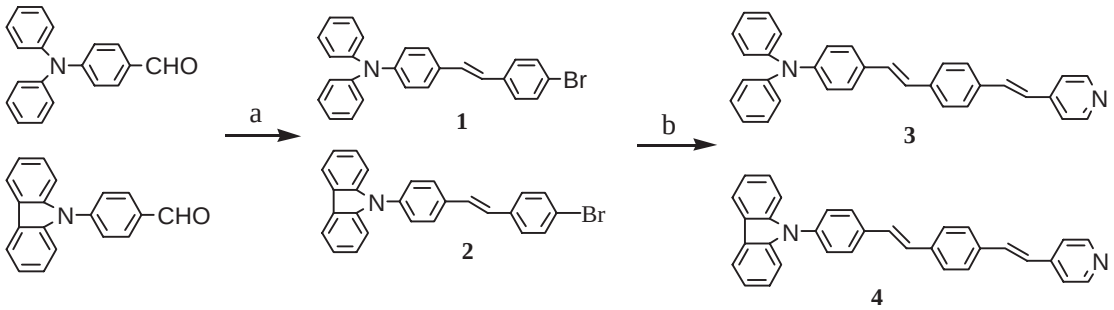

Scheme 1. (a) THF/4-bromobenzyl(triphenyl)phosphonium bromide, room temperature. b) Vinylpyridine/tri-*o*-tolylphosphine/palladium (II) acetate/triethylamine, reflux.

Anal. Calcd for $C_{26}H_{20}NBr$: C, 73.24; H, 4.69; N, 3.29%. Found: C, 73.31; H, 4.75; N, 3.34%. ^{1}H NMR ($CDCl_3$, 600 MHz) δ 7.46 (d, 2H, $J = 8.3$ Hz), 7.36 (m, 4H), 7.27 (t, 4H, $J = 7.7$ Hz), 7.12 (d, 4H, $J = 7.9$ Hz), 7.04 (m, 5H), 6.92 (d, 1H, $J = 16.2$ Hz). ^{13}C NMR (600 MHz, $CDCl_3$) δ 147.78, 147.61, 136.77, 131.78, 131.18, 129.33, 129.09, 127.79, 127.47, 125.81, 124.68, 123.48, 123.21, 120.93.

Diphenyl-(4-{2-[4-(2-pyridin-4-ylvinyl)phenyl]vinyl}phenyl)-amine 3: First, {4-[2-(4-bromophenyl)vinyl]phenyl}diphenylamine (2.13 g, 5 mmol), tri-*o*-tolylphosphine (0.65 g, 2.15 mmol), vinylpyridine (1.16 mL, 10.75 mmol), palladium(II) acetate (0.06 g, 0.27 mmol), and redistilled triethylamine (100 mL) under nitrogen were added to a three-necked flask equipped with a magnetic stirrer, a reflux condenser, and a nitrogen input tube. The reaction mixture was refluxed in an oil bath under nitrogen. An orange product was obtained after heating and stirring for 24 h. The solvent was then removed under reduced pressure and the residue was dissolved in methylene chloride, washed three times with distilled water, and dried with anhydrous magnesium sulfate. It was then filtered and concentrated. The orange compound was purified by column chromatography on silica gel using ethyl acetate/petroleum ether (1:1) as an eluent, and crystallized using ethyl acetate, giving a yield of 60% and mp of 229.0 °C. Anal. Calcd for $C_{33}H_{26}N_2$: C, 88.00; H, 5.78; N, 6.22%. Found: C, 88.15; H, 5.81; N, 6.26%. ^{1}H NMR ($CDCl_3$, 600 MHz) δ 8.59 (d, 2H, $J =$ 4.0 Hz), 7.54 (s, 4H), 7.41 (d, 4H, $J = 8.9$ Hz), 7.30 (m, 4H), 7.14 (d, 4H, $J = 7.7$ Hz), 7.11 (s, 1H), 7.07 (t, 4H, $J = 7.2$ Hz), 7.03 (s, 2H), 7.00 (s, 1H). ^{13}C NMR ($CDCl_3$, 600 MHz) δ 149.55, 147.65, 147.46, 145.25, 138.41, 134.88, 133.33, 131.13, 129.31, 128.98, 127.48, 127.46, 126.72, 126.18, 125.27, 124.62, 123.36, 123.17, 120.90.

9-{4-[2-(4-Bromophenyl)vinyl]phenyl}-9*H*-carbazole 2: It was obtained by a similar method for **1**. The obtained compound was green crystals in a yield of 78%. Anal. Calcd for $C_{26}H_{18}NBr$: C, 73.59; H, 4.28; N, 3.30%. Found: C, 73.71; H, 4.33; N, 3.35%. ^{1}H NMR ($CDCl_3$, 600 MHz) δ 8.14 (d, 2H, $J = 7.8$ Hz), 7.72 (d, 2H, $J = 7.8$ Hz), 7.57 (d, 2H, $J = 7.6$ Hz), 7.51 (d, 2H, $J = 7.6$ Hz), 7.42 (q, 6H, $J = 7.1$ Hz), 7.29 (t, 2H, $J = 7.0$ Hz), 7.16 (q, 2H, $J = 13.9$ Hz).

9-(4-{2-[4-(2-Pyridin-4-ylvinyl)phenyl]vinyl}phenyl)-9*H*-carbazole 4: It was obtained by a similar method for **3**. The obtained green crystals were purified by column chromatography on silica gel using ethyl acetate/petroleum ether (1:1) as an eluent, and crystallized using ethyl acetate in a yield of 58% and mp of 268.4 °C. Anal. Calcd for $C_{33}H_{24}N_2$: C, 88.39; H, 5.36; N, 6.25%. Found: C, 88.22; H, 5.29; N, 6.17%. ^{1}H NMR ($CDCl_3$, 600 MHz) δ 8.61 (d, 2H, $J = 4.3$ Hz), 8.17 (d, 2H, $J = 7.7$ Hz), 7.77 (d, 2H, $J = 7.9$ Hz), 7.60 (m, 6H), 7.45 (m, 6H), 7.30 (m, 4H), 7.09 (s, 1H), 7.06 (s, 1H). ^{13}C NMR ($CDCl_3$, 600 MHz) δ 149.89, 144.92, 140.78, 137.71, 137.13, 136.29, 135.65, 132.95, 128.84, 128.34, 127.89, 127.52, 127.25, 127.08, 125.97, 125.86, 123.48, 120.88, 120.33, 120.04, 109.80.

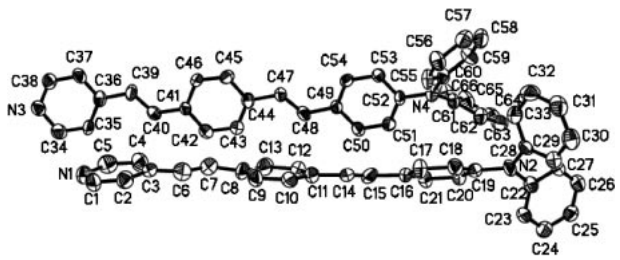

Fig. 1. Crystal structure of **3**.

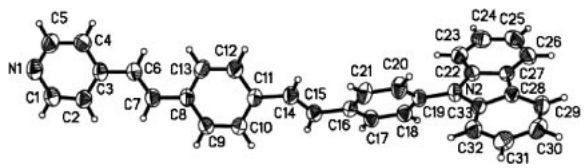

Fig. 2. Crystal structure of **4**.

Results and Discussion

Crystal Structure. The X-ray diffraction data of single crystals for compounds **3** and **4** were collected on a Bruker P4 four-cycle diffractometer with the Mo Kα radiation. Both structures were solved by direct methods, and refined by full-matrix least-squares on F^2 using SHELXL-97 programs.[17] The crystal structures of **3** and **4** are shown in Figs. 1 and 2, respectively. Selected bond distances and bond angles for molecules **3** and **4** are listed in Tables 1 and 2, respectively.[#]

Compound **3** belongs to monoclinic crystal system, $P2_1$ space group, $M = 450.56$, $a = 9.5808(11)$, $b = 8.7128(13)$, $c = 29.489(6)$ Å, $\beta = 93.854(11)$, $V = 2456.1(7)$ Å^3, $Z = 4$, $T = 293(2)$ K, $D_c = 1.218$ g cm^{-3}, $R_1 = 0.0628$, $wR_2 = 0.1122$ for $I > 2\sigma(I)$. Figure 1 shows that there are two molecules in an asymmetric unit. In one molecule, the dihedral angle between C41–C42–C43–C44–C45–C46 and pyridine ring is 11.1°. And the dihedral angle between the former and its adjacent phenyl ring is 9.1°. The dihedral angles between each terminal phenyl ring that links to the N4 atom and C49–C50–C51–C52–C53–C54 are 58.0 and 74.0°, respectively, while that between two terminal phenyl rings is 70.6°. In the

Table 1. Selected Bond Lengths (Å) and Bond Angles (°) for **3**

C1–N1	1.330(12)	C15–C16	1.484(11)	C41–C46	1.413(11)
C1–C2	1.349(11)	C16–C17	1.385(11)	C44–C47	1.478(10)
C2–C3	1.355(13)	C17–C18	1.400(10)	C47–C48	1.325(10)
C3–C4	1.328(13)	C19–N2	1.404(10)	C48–C49	1.478(10)
C3–C6	1.476(14)	C22–N2	1.435(10)	C49–C50	1.405(10)
C4–C5	1.398(13)	C24–C25	1.363(12)	C52–N4	1.429(9)
C5–N1	1.331(13)	C25–C26	1.355(13)	C51–C52	1.379(11)
C6–C7	1.336(13)	C34–N3	1.381(11)	C55–C56	1.357(11)
C7–C8	1.473(13)	C37–C38	1.409(11)	C55–C60	1.387(12)
C8–C13	1.351(14)	C36–C39	1.465(10)	C57–C58	1.380(13)
C8–C9	1.385(14)	C39–C40	1.345(10)	C60–N4	1.410(9)
C11–C14	1.442(11)	C40–C41	1.456(10)	C61–C66	1.375(12)
C14–C15	1.313(11)	C41–C42	1.366(11)	C61–C62	1.367(11)
N1–C1–C2	124.5(12)	C26–C27–C22	120.1(11)	C52–C53–C54	120.3(9)
C1–C2–C3	121.3(11)	C33–C28–N2	119.7(10)	C54–C49–C50	117.3(8)
C4–C3–C2	115.4(10)	C29–C28–N2	121.9(10)	C51–C52–N4	121.5(9)
C4–C3–C6	134.4(13)	C31–C30–C29	119.5(12)	C49–C54–C53	121.8(9)
C2–C3–C6	110.2(11)	C30–C31–C32	121.4(11)	C56–C57–C58	119.1(10)
C3–C4–C5	121.9(12)	C28–C33–C32	121.5(10)	C56–C55–C60	120.8(10)
C6–C7–C8	122.8(11)	C35–C34–N3	122.3(10)	C57–C58–C59	120.7(11)
C9–C8–C7	130.9(13)	C37–C36–C35	115.4(9)	C60–C59–C58	118.8(10)
C13–C12–C11	121.7(11)	N3–C38–C37	123.6(10)	C59–C60–N4	119.3(9)
C15–C14–C11	126.7(11)	C40–C39–C36	125.5(10)	C62–C61–C66	120.4(10)
C14–C15–C16	125.8(11)	C39–C40–C41	127.8(9)	C61–C62–C63	119.2(12)
C16–C21–C20	122.2(10)	C42–C41–C40	120.5(10)	C64–C65–C66	120.2(13)
C25–C24–C23	118.7(10)	C44–C43–C42	121.0(10)	C61–C66–C65	118.9(11)
C23–C22–N2	121.0(9)	C45–C46–C41	120.0(8)	C19–N2–C22	124.3(8)
C16–C21–C20	122.2(10)	C48–C47–C44	127.6(9)	C38–N3–C34	115.6(9)
C26–C25–C24	121.8(10)	C47–C48–C49	125.8(9)	C60–N4–C61	120.5(7)
C25–C26–C27	119.4(10)	C50–C51–C52	121.5(9)	C52–N4–C61	118.8(7)
C2–C3–C6–C7	173.5(11)	C10–C11–C14–C15	169.2(11)	C36–C39–C40–C41	−176.6(9)
C3–C6–C7–C8	−173.4(10)	C11–C14–C15–C16	178.7(10)	C44–C47–C48–C49	−178.5(9)

other molecule, the dihedral angles between C8–C9–C10–C11–C12–C13 and the pyridine ring and adjacent phenyl ring are 10.6 and 22.0°, respectively. Therefore, molecule **3** is almost co-planar. The dihedral angles between each terminal phenyl ring that links to the N2 atom and C16–C17–C18–C19–C20–C21 are 58.4 and 65.1°, respectively, while that between two terminal phenyl rings is 73.2°. The bond lengths of C3–C6, C7–C8, C11–C14, C15–C16, C36–C39, C40–C41, C44–C47, and C48–C49 are shorter than the typical single-bond length of C–C. The bond lengths of C6–C7, C14–C15, C39–C40, and C47–C48 are longer than the typical double-bond length of C=C. These structural features suggest that molecule **3** is a highly delocalized π-electron system.

Compound **4** belongs to a triclinic crystal system, $P\bar{1}$ space group, $M = 448.54$, $a = 9.2893(10)$, $b = 9.6014(17)$, $c = 13.3645(15)$ Å, $\alpha = 92.365(10)$, $\beta = 97.015(6)$, $\gamma = 96.292(10)°$, $V = 1174.1(3)$ Å^3, $Z = 2$, $T = 293$ K, $D_c = 1.269$ g cm^{-3}, $R_1 = 0.0444$, $wR_2 = 0.1010$ for $I > 2\sigma(I)$. Figure 2 shows that the angle between the pyridine ring and the adjacent phenyl ring is only 5.9°. The angle between the two central phenyl rings is 49.2°. The dihedral angle between the carbazole ring and the adjacent phenyl ring is 117.4°. Therefore, molecule **4** is not co-planar. The bridge bond lengths of C3–C6, C7–C8, C11–C14, and C15–C16 are shorter than the typical single bond length of C–C. The bond lengths of C6–C7 and C14–C15 are longer than the typical double bond length of C=C. The conjugated geometric configuration reveals that molecule **4** is also a highly delocalized π-electron system.

Linear Absorption and Fluorescence Spectra. The photophysical properties of **3** and **4** are summarized in Table 3. The one-photon fluorescence spectra and lifetimes of these two compounds were measured in different solvents with a concentration of $c = 1 \times 10^{-5}$ mol/L. The excited wavelengths of **3** and **4** were 400 and 366 nm, respectively. The two-photon induced emission spectrum could be observed with a suitable laser beam from a mode-locked Ti:sapphire laser (Coherent Mira 900F) as the pump source with a pulse duration of 200 fs, a repetition rate of 76 MHz, and a single-scan streak camera (Hamamatsu Model C5680-01) together with a monochromator as the recorder. The TPA induced emission spectra of two compounds were measured in different solvents with a concentration of $c = 1 \times 10^{-2}$ mol/L. The excited wavelengths of compounds **3** and **4** were 800 and 760 nm, respectively. Figures 3, 4, and 5 show the linear absorption, one- and two-photon fluorescence spectra of compounds **3** and **4** in $CHCl_3$. As shown in Table 3, the maximum absorption show a slight blue-shift, while the maximum fluorescence clearly show red-shifts, and lengthened fluorescent lifetimes, except for benzyl alcohol, along with increase in the polarity

Table 2. Selected Bond Lengths (Å) and Bond Angles (°) for **4**

C1–N1	1.333(2)	C11–C12	1.391(2)	C22–C27	1.411(2)
C1–C2	1.375(2)	C11–C14	1.467(2)	C23–C24	1.373(3)
C2–C3	1.388(2)	C12–C13	1.371(2)	C24–C25	1.392(3)
C3–C4	1.389(3)	C14–C15	1.319(2)	C25–C26	1.372(3)
C3–C6	1.462(2)	C15–C16	1.467(2)	C26–C27	1.392(2)
C4–C5	1.378(2)	C16–C17	1.388(2)	C27–C28	1.441(2)
C5–N1	1.322(2)	C16–C21	1.392(2)	C28–C29	1.400(2)
C6–C7	1.321(3)	C17–C18	1.381(2)	C28–C33	1.409(2)
C7–C8	1.469(2)	C18–C19	1.378(2)	C29–C30	1.374(3)
C8–C13	1.389(2)	C19–C20	1.377(2)	C30–C31	1.392(3)
C8–C9	1.391(2)	C19–N2	1.4326(19)	C31–C32	1.376(2)
C9–C10	1.374(2)	C20–C21	1.372(2)	C32–C33	1.383(2)
C10–C11	1.391(2)	C22–N2	1.391(2)	C33–N2	1.392(2)
N1–C1–C2	124.50(19)	C15–C14–C11	127.40(17)	C25–C26–C27	119.58(18)
C1–C2–C3	119.81(18)	C14–C15–C16	125.26(17)	C26–C27–C22	118.72(17)
C2–C3–C4	115.80(16)	C17–C16–C21	117.37(15)	C26–C27–C28	134.48(16)
C2–C3–C6	124.40(18)	C17–C16–C15	120.60(15)	C22–C27–C28	106.80(14)
C4–C3–C6	119.78(17)	C21–C16–C15	121.99(16)	C29–C28–C33	118.35(17)
C5–C4–C3	119.83(19)	C18–C17–C16	121.66(16)	C29–C28–C27	134.68(16)
N1–C5–C4	124.6(2)	C19–C18–C17	119.85(16)	C33–C28–C27	106.95(15)
C7–C6–C3	126.94(18)	C20–C19–C18	119.21(15)	C30–C29–C28	119.71(17)
C6–C7–C8	126.12(18)	C20–C19–N2	120.11(15)	C29–C30–C31	120.55(18)
C13–C8–C9	117.19(16)	C18–C19–N2	120.68(15)	C32–C31–C30	121.42(19)
C13–C8–C7	122.30(17)	C21–C20–C19	120.91(16)	C31–C32–C33	117.95(17)
C9–C8–C7	120.51(16)	C20–C21–C16	120.99(17)	C32–C33–N2	129.15(15)
C10–C9–C8	121.97(17)	N2–C22–C23	129.29(16)	C32–C33–C28	122.01(16)
C9–C10–C11	120.52(17)	N2–C22–C27	108.83(15)	N2–C33–C28	108.79(15)
C12–C11–C10	117.51(15)	C23–C22–C27	121.84(17)	C5–N1–C1	115.36(17)
C12–C11–C14	118.92(16)	C24–C23–C22	117.41(18)	C22–N2–C33	108.61(13)
C10–C11–C14	123.56(16)	C23–C24–C25	121.8(2)	C22–N2–C19	125.83(15)
C13–C12–C11	121.67(17)	C26–C25–C24	120.61(19)	C33–N2–C19	125.55(15)
C4–C3–C6–C7	169.2(2)	C12–C11–C14–C15	−152.1(2)	N2–C22–C23–C24	179.38(18)
C3–C6–C7–C8	−177.93(17)	C11–C14–C15–C16	176.07(17)	C31–C32–C33–N2	178.36(16)

Table 3. The Data of Absorption, One- and Two-Photon Fluorescence Spectra with Solvent Effects of **3** and **4**

Compds	Solvents	ε	$\lambda_{max}^{(1a)}$/nm	$\varepsilon_{res}/10^4$	$\lambda_{max}^{(1f)}$/nm	τ/ns	Φ	$\lambda_{max}^{(2)}$/nm
3	DMF	37.6	397	5.76	570	2.44	0.84	559
	CH_2Cl_2	9.1	399	4.80	540	2.19	0.73	542
	Benzyl alcohol	13.1	409	4.28	558	2.11	0.97	574
	THF	7.58	398	5.39	536	1.93	0.66	538
	$CHCl_3$	4.806	401	4.66	520	1.74	0.68	523
4	DMF	37.6	364	6.63	485	1.81	0.80	487
	CH_2Cl_2	9.1	366	6.33	470	1.47	0.66	482
	Benzyl alcohol	13.1	375	5.92	482	1.60	0.89	493
	THF	7.58	365	6.54	468	1.37	0.56	478
	$CHCl_3$	4.806	367	6.39	457	1.22	0.58	473

$\lambda_{max}^{(1a)}$, $\lambda_{max}^{(1f)}$, and $\lambda_{max}^{(2)}$ are one-photon absorption, one-photon fluorescence, and two-photon fluorescence maxima peak, respectively. Φ is one–photo quantum yield determined using coumarin 307 as the standard.[21] τ is one-photon fluorescence lifetime. ε is the relative permittivity that was measured at 20 °C.[22] ε_{res} is the corresponding molar absorption coefficient.

of the solvent for each compound. The fact can be explained because the excited states of these compounds may possess higher polarity than that of the ground states, since the solvatochromism is associated with energy-level lowering. An increased dipole-dipole interaction between the solute and the solvent would lead to a great lowering of the energy-level.[18,19] For the case of benzyl alcohol, we can easily realize the possibility of hydrogen bonding formation between the solvent and solute molecules, which would push the excitation energy lower.[15] It is should noted that both the largest one-photon oscillator strength and the maximum two-photon absorption cross section take place in the same excited state, the charge

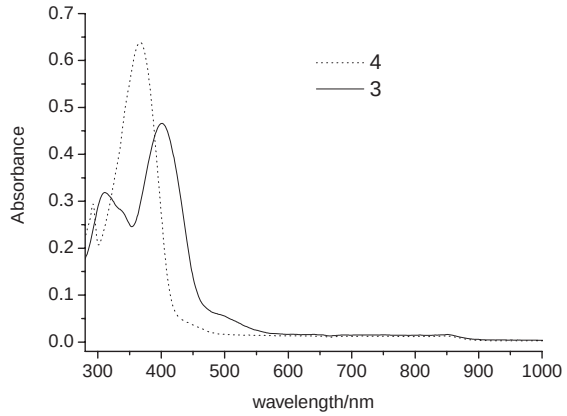

Fig. 3. Linear absorption spectra of **3** and **4** in $CHCl_3$ with a concentration of $c = 1 \times 10^{-5}$ mol/L.

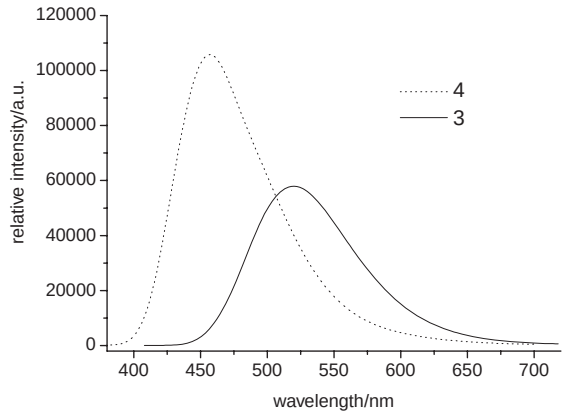

Fig. 4. One-photon fluorescence spectra of **3** and **4** in $CHCl_3$ with a concentration of $c = 1 \times 10^{-5}$ mol/L.

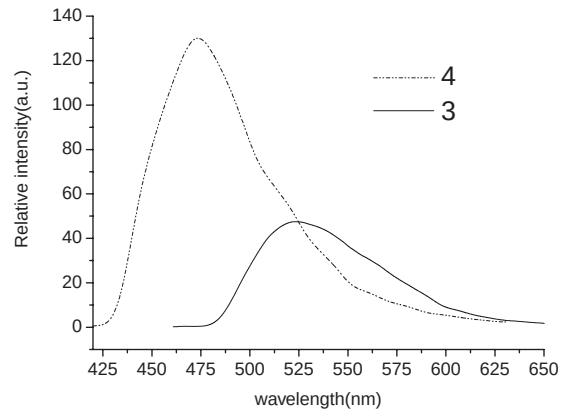

Fig. 5. Two-photon fluorescence spectra of **3** and **4** in $CHCl_3$ with a concentration of $c = 1 \times 10^{-2}$ mol/L.

transfer state, in the lower energy region, because of the asymmetrical characteristics of the present molecules. Therefore, we studied the two-photon fluorescence spectra, as described in the following section.[20] Comparing compound **3** with **4**, we can see that replacing of the carbazolyl by the diphenylamino group resulted in an enhancement of the one-photon quantum yield and a red-shift of the absporption and emission band. This may provide evidence that the electron-donating strength of diphenylamino group is greater than that of carbazolyl group, which increases the charge transfer character.

In addition to the similarities between one-photon fluorescence and two-photon fluorescence, the two-photon fluorescence peak positions are also independent of the laser wavelength used. Thus, although the electrons can be pumped to the different excited states by linear absorption, or two-photon absorption, due to the different selection rules, they would finally relax to the same lowest excited state via internal conversion and/or vibrational relaxation.

Two-Photon Absorption Cross-Sections. The transition intensity for one-photon absorption (OPA) is described by the oscillator strength,

$$\delta_{\mathrm{op}} = \frac{2\omega_f}{3} \sum_{\alpha} |\langle 0|\mu_\alpha|f\rangle|^2, \tag{1}$$

where μ_α is the electric dipole moment operator, ω_f denotes the excitation energy of the excited state $|f\rangle$, $\langle 0|$ denotes the ground state, and the summation is performed over the molecular x, y, and z axes.

In terms of sum-over-state formula, the two-photon matrix element for the two-photon resonant absorption of identical energy is written as

$$S_{\alpha\beta} = \sum_j \left[\frac{\langle 0|\mu_\alpha|j\rangle\langle j|\mu_\beta|f\rangle}{\omega_j - \omega_f/2} + \frac{\langle 0|\mu_\beta|j\rangle\langle j|\mu_\alpha|f\rangle}{\omega_j - \omega_f/2} \right], \tag{2}$$

where $\langle 0|$ and $|f\rangle$ denote the ground state and the final state, respectively; $|j\rangle$ means all of the intermediate states, including the ground state; ω_j is the excitation energy of the excited state $|j\rangle$. The TPA cross section is given by orientational averaging over the two-photon absorption probability,

$$\delta_{\mathrm{tpa}} = \sum_{\alpha\beta} \left[F \times S_{\alpha\alpha} S^*_{\beta\beta} + G \times S_{\alpha\beta} S^*_{\alpha\beta} + H \times S_{\alpha\beta} S^*_{\beta\alpha} \right], \tag{3}$$

where the coefficients F, G, and H are related to the incident radiation. For linearly polarized light, F, G, and H are 2, 2, and 2, but for the circular case, they are -2, 3, and 3, respectively. In the present work, we only considered the results with a linearly polarized laser beam. The summation goes over the molecular axes $\alpha, \beta = \{x, y, z\}$.

The TPA cross section, which is directly comparable with experimental measurements, is defined as

$$\sigma_{\mathrm{tpa}} = \frac{4\pi^2 a_0^5 \alpha}{15 c_0} \frac{\omega^2 g(\omega)}{\Gamma_f} \delta_{\mathrm{tpa}}, \tag{4}$$

where a_0 is the Bohr radius, c_0 the speed of light, α the fine structure constant, $\hbar\omega$ the photon energy of the incident light; $g(\omega)$ denotes the spectral line profile, and here it is assumed to be a δ function. Γ_f is the lifetime broadening of the final state, which is assumed to be 0.1 eV.[11]

We utilized the GAUSSIAN-98 program package[23] to optimize the molecular geometrical structure with hybrid density functional theory (DFT/B3LYP) and a basis set 6-31G. The excited energies for two molecules are then calculated by time-dependent density functional theory. The first excited energies for molecules **3** and **4** are 466 and 428 nm, respectively.

The program DALTON[24] was used to study the two-photon absorption cross sections of the two molecules. For the first ex-

cited state, the TPA cross sections (σ, 10^{-50} cm^4 s photon^{-1}) for molecules **3** and **4**, irradiated with the linearly polarized laser, were 59.3 and 43.0, respectively, which indicate that both of the two molecules have a relatively large two-photon absorption cross section under the experimental circumstance. Therefore, these two molecules can be used as two-photon polymerization initiators.

Two-Photon Photopolymerization. In our two-photon initiation polymerization experiments, two-dimensional cross-linked periodic microstructures were fabricated with a negative resins system, which contained oligomer (bisphenyl A epoxide dimethylacrylate) and 0.5% of compound **3** or **4** as an initiator and a little 1,2-dichloroethane (increasing the compatibility and controlling the viscosity). The excited wavelengths for initiating two-photon polymerization reactions of **3** and **4** were 800 and 760 nm, respectively. The same mode-locked Ti:sapphire laser as that used in the two-photon fluorescence measurements was used for two-photon microfabircation. The lasing source was tightly focused via an objective lens ($\times$40, NA = 0.65), and the focal point was focused on a sample film on an *xy*-step monitorized stage controlled by a computer. The pulse energy after being focused by the objective lens was $\sim$20 mW. The polymerized solid skeleton was obtained after the unreacted liquid mixture had been washed out. The fabricated lattice was observed through a polarization microscope (Olympus, BX-51). Its photograph is illustrated in Fig. 6.

The photopolymerization mechanisms of these two initiators are still unknown. According to Cumpston et al.,[2] strong donor substituents would make the conjugated system electron rich, and after one- or two-photon photoexcitation, these chromophores would be able to transfer an electron even to relatively weak acceptors. This process could be used to activate the polymerization reaction. In order to demonstrate this process, we tried to conduct a theoretical investigation. Our ab initio calculation using time-dependent hybrid density functional theory B3LYP level coded in a GAUSSIAN package for the molecule **3** showed that the first excited state was the charge transfer (CT) state with an excited energy $\lambda = 466$ nm ($\Delta E = 2.6589$ eV, $f = 1.2563$). When the molecule was irradiated by a 800 nm laser beam, it could be expected that the molecule would simultaneously absorb two photons, and be excited to the first excited state (the CT state). We plotted

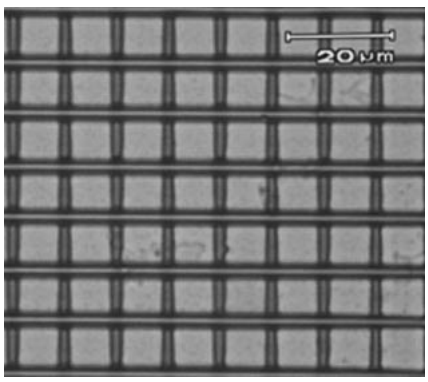

Fig. 6. Optical micrograph of the lattice fabricated via two-photon polymerization using **3** as an initiator.

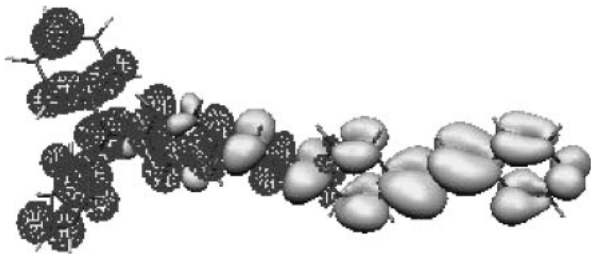

Fig. 7. Density difference between the charge-transfer and ground states of molecule **3** in gas phase. Areas with chickenwire and dots represent the electron lose and gain, respectively, upon the excitation.

the charge-density difference between the ground and the CT states for **3** in the gas phase (see Fig. 7), which was visualized using the MOLEKEL program.[25] Figure 7 shows that upon excitation, charges were mainly transferred from the acceptor side to the donor side of the molecule. In the CT state, there were more electrons at the donor side, indicating that the molecule could give away its electron to its surroundings. This picture seems to support Cumpston's conclusion.[2] However, whether the photoinduced electron-transfer reaction can be energetically feasible needs to be further investigated theoretically.

Conclusion

Two new two-photon photopolymerization initiators of **3** and **4** were synthesized and characterized. The one-photon fluorescence quantum yields, lifetimes, and solvent effects of the initiators were studied in detail, and both compounds exhibit a large delocalized π-electron conjugated system. The experimental results suggest that they are good two-photon absorbing chromophores and effective two-photon photopolymerization initiators. The two-photon absorption cross sections of them were calculated, and two-photon initiation polymerization experiments were carried out. The possible photopolymerization mechanism was considered for the case when laser irradiation is applied.

This work was supported by grants from the financial support of the state National Natural Science Foundation of China (grant no. 50323006, 50325311, 10274044) and Swedish International Development Cooperation Agency (Sida).

References

See http://www.rsc.org/CCDC 234127 and 234128.

1 S. Maruo, O. Nakamura, and S. Kawata, *Opt. Lett.*, **22**, 132 (1997).

2 B. H. Cumpston, S. P. Ananthavel, S. Barlow, D. L. Dyer, J. E. Ehrlich, L. L. Erskine, A. A. Keikal, S. M. Kuebler, I.-Y. S. Lee, D. M. Maughon, J. Qin, H. Röckel, M. Rumi, X. L. Wu, S. R. Marder, and J. W. Perry, *Nature*, **398**, 51 (1999).

3 S. Kawata, H.-B. Sun, T. Tanaka, and K. Takada, *Nature*, **412**, 697 (2001).

4 S. Maruo and K. Ikuta, *Proc. Soc. Photo-Opt. Instrum. Eng.*, **3937**, 106 (2000).

5 V. Mizeikis, S. Juodkazis, A. Marcinkevičius, S. Matsuo, and H. Misawa, *J. Photochem. Photobiol., C*, **2**, 35 (2001).

6 H.-B. Sun, S. Matsuo, and H. Misawa, *Appl. Phys. Lett.*,

74, 786 (1999).

7 H. E. Pudavar, M. P. Joshi, P. N. Prasad, and B. A. Reinhardt, *Appl. Phys. Lett.*, **74**, 1338 (1999).

8 W. Denk, *Proc. Natl. Acad. Sci. U.S.A.*, **91**, 6629 (1994).

9 R. M. Williams, D. W. Piston, and W. W. Webb, *Fed. Am. Soc. Exp. Biol. J.*, **8**, 804 (1994).

10 S. M. Kuebler, B. H. Cumpson, S. Ananthavel, S. Barlow, J. E. Ehrlich, L. L. Etsine, A. A. Heikal, D. McCord-Maughon, J. Qin, H. Rocel, M. Rumi, S. R. Marder, and J. W. Perry, *SPIE-Int. Soc. Opt. Eng.*, **3937**, 97 (2000).

11 M. Albota, D. Beljonne, J.-L. Brédas, J. E. Ehrlich, J.-Y. Fu, A. A. Heikal, S. E. Hess, T. Kogej, M. D. Levin, S. R. Marder, D. McCord-Maughon, J. W. Perry, H. Röckel, M. Rumi, G. Subramaniam, W. W. Webb, X.-L. Wu, and C. Xu, *Science*, **281**, 1653 (1998).

12 B. A. Reinhardt, L. L. Brott, S. J. Clarson, A. G. Dillard, J. C. Bhatt, R. Kannan, L. Yuan, G. S. He, and P. N. Prasad, *Chem. Mater.*, **10**, 1863 (1998).

13 M. Rumi, J. E. Ehrlich, A. A. Heikal, J. W. Perry, S. Barlow, Z. Hu, D. M. Maughon, T. C. Parker, H. Rockel, S. Thayumanavan, S. R. Marder, D. Beljonne, and J.-L. Bredas, *J. Am. Chem. Soc.*, **122**, 9500 (2000).

14 Y. Ren, X.-Q. Yu, D.-J. Zhang, D. Wang, M.-L. Zhang, G.-B. Xu, X. Zhao, Y.-P. Tian, Z.-S. Shao, and M.-H. Jiang, *J. Mater. Chem.*, **12**, 3431 (2002).

15 C.-K. Wang, P. Macak, Y. Luo, and H. Ågren, *J. Chem. Phys.*, **114**, 9813 (2001).

16 X.-M. Wang, Y.-F. Zhou, W.-T. Yu, C. Wang, Q. Fang, M.-H. Jiang, H. Lei, and H.-Z. Wang, *J. Mater. Chem.*, **10**, 2698 (2000).

17 G. M. Sheldrick, Program for the Refinement of Crystal Structures, University of Göttingen, Germany, 1997.

18 P. Fromherz, *J. Phys. Chem.*, **99**, 7188 (1995).

19 U. Narang, C. F. Zhao, J. D. Bhawalkar, F. V. Bright, and P. N. Prasad, *J. Phys. Chem.*, **100**, 4521 (1996).

20 C.-K. Wang, Y.-H Wang, Y. Su, and Y. Luo, *J. Chem. Phys.*, **119**, 4409 (2003).

21 J. N. Demas and G. A. Crosby, *J. Phys. Chem.*, **75**, 991 (1971).

22 "CRC Handbook of Chemistry and Physics," ed by D. R. Lide, CRC Press, Boca Raton, FL, 73rd edu., 1992–1993.

23 GAUSSIAN98, References in http://www.gaussian.com.

24 T. Helgaker et al., DALTON, An ab initio electronic structure program, Release 1.0 (1997). See http://www.kjemi.uio.no/software/dalton/dalton.html.

25 MOLEKEL, References in http://www.cscs.ch/molekel/.